PROCEEDINGS OF SCIENCE

Ergoregion instability of black hole mimickers

Paolo Pani*
Dipartimento di Fisica, Università di Cagliari, and INFN sezione di Cagliari, Cittadella Universitaria 09042 Monserrato, Italy †
E-mail: paolo.pani@ca.infn.it

Vitor Cardoso
Centro Multidisciplinar de Astrofísica - CENTRA, Dept. de Física, Instituto Superior Técnico, Av. Rovisco Pais 1, 1049-001 Lisboa, Portugal
Department of Physics and Astronomy, The University of Mississippi, University, MS 38677-1848, USA
E-mail: vcardoso@fisica.ist.utl.pt

Mariano Cadoni
Dipartimento di Fisica, Università di Cagliari, and INFN sezione di Cagliari, Cittadella Universitaria 09042 Monserrato, Italy
E-mail: mariano.cadoni@ca.infn.it

Marco Cavaglià
Department of Physics and Astronomy, The University of Mississippi, University, MS 38677-1848, USA
E-mail: cavaglia@phy.olemiss.edu

Ultra-compact, horizonless objects such as gravastars, boson stars, wormholes and superspinars can mimick most of the properties of black holes. Here we show that these "black hole mimickers" will most likely develop a strong ergoregion instability when rapidly spinning. Instability timescales range between $\sim 10^{-5}$s and $\sim$ weeks depending on the object, its mass and its angular momentum. For a wide range of parameters the instability is truly effective. This provides a strong indication that astrophysical ultra-compact objects with large rotation are black holes.

Black Holes in General Relativity and String Theory
August 24-30 2008
Veli Lošinj,Croatia

*Speaker.
†Presently at Centro Multidisciplinar de Astrofísica - CENTRA, Dept. de Física, Instituto Superior Técnico, Av. Rovisco Pais 1, 1049-001 Lisboa, Portugal

PoS(BHs, GR and Strings)027

1. Introduction

Black holes (BHs) in Einstein-Maxwell theory are characterized by three parameters [1]: mass M, electric charge Q and angular momentum $J \equiv aM \leqslant M^2$. BHs are thought to be abundant objects in the Universe. Their mass is estimated to vary between $3M_\odot$ and $10^{9.5}M_\odot$ or higher [2], their electrical charge is negligible because of the effect of surrounding plasma [3] and their angular momentum is expected to be close to the extremal limit because of accretion and merger events [4]. A non-comprehensive list of some astrophysical BH candidates [2, 5, 6, 7] is shown in Table 1.

Table 1: Mass, M, radius, R, angular momentum, J, and compactness, $\mu = M/R$, for some BH candidates (from [2, 5, 6, 7])

Candidate	**Mass** ($M_\odot$)	**Radius** ($R_\odot$)	J/M^2	**Compactness** $\mu = M/R$
GRO J1655-40	6.3	$(1.6-2.6)\times 10^{-5}$	$0.65-0.80$	$0.47-0.83$
XTE J1550-564	10	$(2.1-8.4)\times 10^{-5}$	$0.90-1.00$	$0.25-0.99$
GRS 1915+105	14	$(2.9-9.7)\times 10^{-5}$	$0.98-1.00$	$0.30-0.99$
SGR A*	4×10^6	$\lesssim 27$	$0.50-1.00$	$\gtrsim 0.31$

Despite the wealth of circumstantial evidence, there is no definite observational proof of the existence of astrophysical BHs due to the difficulty to detect an event horizon in astrophysical BH candidates [2, 8]. Thus astrophysical objects without event horizon, yet observationally indistinguishable from BHs, cannot be excluded a priori. Some of the most viable alternative models describing an ultra-compact astrophysical object include gravastars, boson stars, wormholes and superspinars.

Dark energy stars or *gravastars* are compact objects with de Sitter interior and Schwarzschild exterior [9]. These two regions are glued together by a model-dependent intermediate region. In the original model [9] the intermediate region is an ultra-stiff thin shell. Models without shells or discontinuities have also been investigated [10, 11].

Boson stars are macroscopic quantum states which are prevented from undergoing complete gravitational collapse by Heisenberg uncertainty principle [12]. Their models differ in the scalar self-interaction potential which also set the allowed maximum compactness for a boson star.

An exhaustive description of *wormholes* can be found in the monograph [13] (see also Ref. [14]). In this work we shall consider particular wormholes which are infinitesimal variations of BH spacetimes. These wormholes may be indistinguishable from ordinary BHs [15].

Superspinars are solutions of the gravitational field equations that violate the Kerr bound. These geometries could be created by high energy corrections to Einstein gravity such as those present in string-inspired models [16].

The objects described above can be almost as compact as a BH and thus they are virtually indistinguishable from BHs in the Newtonian regime, hence the name "BH mimickers". Although exotic these objects provide viable alternatives to astrophysical BHs. BH mimickers being horizonless, no information loss paradox [17] arises in these spacetimes. Moreover they can be regular at the origin, avoiding the problem of singularities. By Birkhoff's theorem, the vacuum exterior of a spherically symmetric object is described by the Schwarzschild spacetime. Thus the motion

of orbiting objects both around a static BH and around a static ultra-compact object is the same and it makes virtually impossible to discern between a Schwarzschild BH and a static neutral BH mimicker. Instead for rotating objects deviations in the properties of orbiting objects occur. Since BH mimickers are very compact these deviations occur close to the horizon and are not easily detectable electromagnetically. To ascertain the true nature of ultra-compact objects it is thus important to devise observational tests to distinguish rotating BH mimickers from ordinary Kerr BHs. The traditional way to distinguish a BH from a neutron star is to measure its mass. If the latter is larger than the Chandrasekhar limit, the object is believed to be a BH. However, this method cannot be used for the BH mimickers discussed above, because of their broad mass spectrum. The main difference between a BH and a BH mimicker is the presence of an event horizon in the former. Some indirect experimental methods to detect the event horizon has been proposed [18, 19]. Another very promising observational method to probe the structure of ultra-compact objects is gravitational wave astronomy. From the gravitational waveform it is expected to detect the presence of an event horizon in the source [20]. Some other BH mimickers (for example electrically charged quasi-BHs [21]) are already ruled out by experiments. Moreover there are evidences that some model for BH mimickers is plagued by a singular behavior in the near-horizon limit [22].

Here, we describe a method originally proposed in [23, 24] for discriminating rotating BH mimickers from ordinary BHs. This method uses the fact that compact rotating objects without event horizon are unstable when an ergoregion is present. This *ergoregion instability* appears in any system with ergoregions and no horizons [25]. The origin of this instability can be traced back to superradiant scattering. In a scattering process, superradiance occurs when scattered waves have amplitudes larger than incident waves. This leads to extraction of energy from the scattering body [26, 27, 28]. Instability may arise whenever this process is allowed to repeat itself ad infinitum. This happens, for example, when a BH is surrounded by a "mirror" that scatters the superradiant wave back to the horizon, amplifying it at each scattering, as in the *BH bomb* process [29, 30]. If the mirror is inside the ergoregion, superradiance may lead to an inverted BH bomb. Some superradiant waves escape to infinity carrying positive energy, causing the energy inside the ergoregion to decrease and eventually generating an instability. This may occur for any rotating star with an ergoregion: the mirror can be either its surface or, for a star made of matter non-interacting with the wave, its center. On the other hand BHs could be stable due to the absorption by the event horizon being larger than superradiant amplification. Indeed Kerr BHs are stable aganist small scalar, electromagnetic and gravitational perturbations [31].

Rapidly rotating stars do possess an ergoregion and thus they are unstable. However typical instability timescales are shown to be larger than the Hubble time [32]. Thus the ergoregion instability is too weak to produce any effect on the evolution of stars. This conclusion changes drastically for BH mimickers due to their compactness [23, 24]. For some of the rotating BH mimickers described above, instability timescales range between $\sim 10^{-5}$s and $\sim$ weeks depending on the object, its mass and its angular momentum.

This paper is organized as follows. In Section 2 we deal with gravastars and boson stars. We describe rotating models for these objects and discuss their instability timescale. In Section 3 a toy model for both rotating wormholes and superspinars is presented. Section 4 contains a brief discussion of the results and concludes the paper. Throughout the paper geometrized units ($G = c = 1$) are used, except during the discussion of results for rotating boson stars when we set

the Newton constant to be $G = 0.05/(4\pi)$ as in Ref. [33].

2. Gravastars and boson stars

This section discusses the main properties of gravastars and boson stars as well as the method to compute the ergoregion instability for these objects. For a more detailed discussion see [23].

2.1 Nonrotating Gravastars

Although exact solutions for spinning gravastars are not known, they can be studied in the limit of slow rotation by perturbing the nonrotating solutions [34]. This procedure was used in Ref. [35] to study the existence of ergoregions for ordinary rotating stars with uniform density. In the following, we omit the discussion for the original thin-shell model by Mazur and Mottola [9] and we focus on the anisotropic fluid model by Chirenti and Rezzolla [10, 11].

The model assumes a thick shell with continuous profile of anisotropic pressure to avoid the introduction of an infinitesimally thin shell. The stress-energy tensor is $T^{\mu}{}_{\nu} = \mathrm{diag}[-\rho, p_r, p_t, p_t]$, where p_r and p_t are the radial and tangential pressures, respectively. The spherical symmetric metric is

$$ds^2 = -f(r)dt^2 + B(r)dr^2 + r^2 d\Omega_2^2 \tag{2.1}$$

and it consists of three regions: an interior ($r < r_1$) described by a de Sitter metric, an exterior ($r > r_2$) described by the Schwarzschild metric and a model-dependent intermediate ($r_1 < r < r_2$) region. In the following we shall indicate with $\delta = r_2 - r_1$ the thickness of the intermediate region and with $\mu = M/r_2$ the compactness of the gravastar. In the model by Chirenti and Rezzolla the density function is

$$\rho(r) = \begin{cases} \rho_0\,, & 0 \le r \le r_1 & \text{interior} \\ ar^3 + br^2 + cr + d\,, & r_1 < r < r_2 & \text{intermediate} \\ 0\,, & r_2 \le r & \text{exterior} \end{cases}$$

where a, b, c and d are found imposing continuity conditions $\rho(0) = \rho(r_1) = \rho_0$, $\rho(r_2) = \rho'(r_1) = \rho'(r_2) = 0$ and ρ_0 is found fixing the total mass, M. The metric coefficients are

$$f = \left(1 - \frac{2M}{r_2}\right) e^{\Gamma(r) - \Gamma(r_2)}\,, \quad \frac{1}{B} = 1 - \frac{2m(r)}{r}\,, \tag{2.2}$$

where

$$m(r) = \int_0^r 4\pi r^2 \rho\, dr\,, \qquad \Gamma(r) = \int_0^r \frac{2m(r) + 8\pi r^3 p_r}{r(r - 2m(r))} dr\,. \tag{2.3}$$

The above equations and some closure relation, $p_r = p_r(\rho)$, completely determine the structure of the gravastar [10]. The behaviors of the metric coefficients for a typical gravastar are shown in Fig. 1.

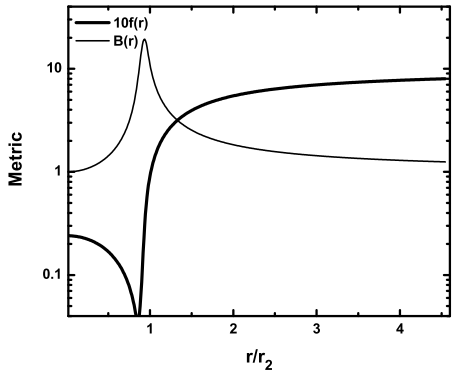

Figure 1: Metric coefficients for the anisotropic pressure model ($r_2 = 2.2$, $r_1 = 1.8$ and $M = 1$).

2.1.1 Slowly rotating gravastars and ergoregions

Slowly rotating solutions can be obtained using the method developed in Ref. [34]. A rotation of order Ω gives corrections of order Ω^2 in the diagonal coefficients of the metric (2.1) and introduces a non-diagonal term of order Ω, $g_{t\phi} \equiv -\omega g_{\phi\phi}$, where ϕ is the azimuthal coordinate and $\omega = \omega(r)$ is the angular velocity of frame dragging. The full metric is

$$ds^2 = -f(r)dt^2 + B(r)dr^2 + r^2 d\theta^2 + r^2 \sin^2\theta \left(d\phi - \omega(r)dt\right)^2 . \tag{2.4}$$

If the gravastar rotates rigidly, i.e. $\Omega = \text{constant}$, from the (t,ϕ) component of Einstein equations we find a differential equation for $\omega(r)$ [23]

$$\omega'' + \omega' \left(\frac{4}{r} + \frac{j'}{j}\right) = 16\pi B(r)(\omega - \Omega)(\rho + p_t) , \tag{2.5}$$

where $j \equiv (fB)^{-1/2}$ is evaluated at zeroth order and ρ, p_t are given in terms of the nonrotating geometry. The above equation reduces to the corresponding equation for isotropic fluids [34]. Solutions of Eq. (2.5) describe rotating gravastars to first order in Ω.

The ergoregion can be found by computing the surface on which g_{tt} vanishes [35]. An approximated relation for the location of the ergoregion in very compact gravastars is

$$0 = -f(r) + \omega^2 r^2 \sin^2\theta . \tag{2.6}$$

The existence and the boundaries of the ergoregions can be computed from the above equations. We integrate equation (2.5) from the origin with initial conditions $(\Omega - \omega)' = 0$ and $(\Omega - \omega)$ finite. The exterior solution satisfies $\omega = 2J/r^3$, where J is the angular momentum of the gravastar. Demanding the continuity of both $(\Omega - \omega)'$ and $(\Omega - \omega)$, Ω and J are uniquely determined. The rotation parameter Ω depends on the initial condition at the origin. Figure 2 shows the results the gravastar model described in the previous sections. The ergoregion can be located by drawing an horizontal line at the desired value of J/M^2. The minimum of the curve is the minimum values of J/M^2 which are required for the existence of the ergoregion. Comparison with the results for stars

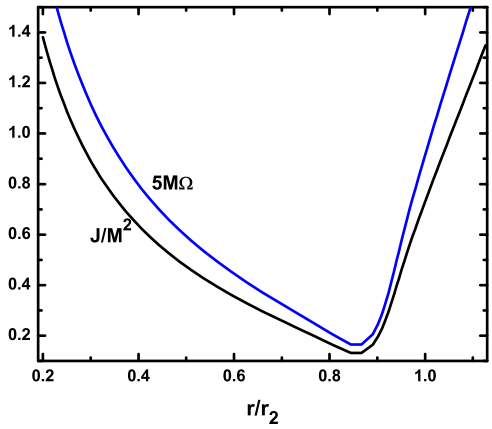

Figure 2: J/M^2 and angular frequency Ω for the anisotropic pressure model with $r_2 = 2.2$, $r_1 = 1.8$ and $M = 1$.

of uniform density [35], shows that ergoregions form more easily around gravastars due to their higher compactness. The slow-rotation approximation is considered valid for $\Omega/\Omega_K < 1$ where $M\Omega_K = \mu^{3/2}$ is the Keplerian frequency.

Depending on the compactness, μ, the angular momentum, J, and the thickness, δ, a spinning gravastar does or does not develop an ergoregion. The formation of an ergoregion for rotating gravastar is exhaustively discussed in the whole parameters space in Ref. [36]. A delicate issue is the strong dependence on the thickness, δ, which cannot be directly measured by experiments. Figure 3 shows how the ergoregion width is sensitive to δ.

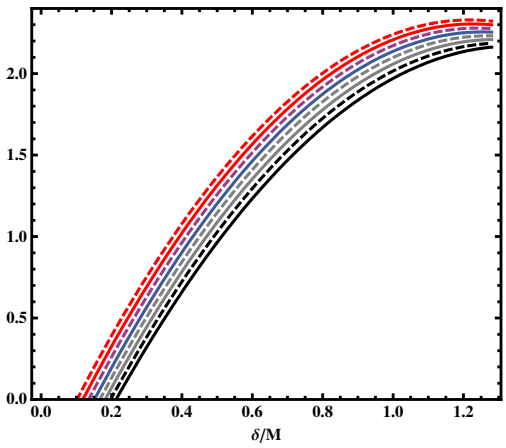

Figure 3: Ergoregion width (in units of M) as function of the thickness, $\delta = r_2 - r_1$, for $r_2 = 2.3$, $M = 1$ and for different J values. From top to bottom: $J/M^2 = 0.95$, 0.90, 0.85, 0.80, 0.75, 0.70, 0.65 and 0.60. The ergoregion width decreases as $\delta \to 0$.

2.2 Rotating boson stars

A example of rotating boson star is the model by Kleihaus, Kunz, List and Schaffer (KKLS) [33]. The KKLS solution is based on the Lagrangian for a self-interacting complex scalar field

$$\mathscr{L}_{KKLS} = -\frac{1}{2} g^{\mu\nu} \left(\Phi^*_{,\mu} \Phi_{,\nu} + \Phi^*_{,\nu} \Phi_{,\mu} \right) - U(|\Phi|), \tag{2.7}$$

where $U(|\Phi|) = \lambda |\Phi|^2 (|\Phi|^4 - a|\Phi|^2 + b)$. The mass of the boson is given by $m_{\rm B} = \sqrt{\lambda b}$. The ansatz for the axisymmetric spacetime is

$$ds^2 = -f dt^2 + \frac{k}{f} \left[g \left(dr^2 + r^2 d\theta^2 \right) + r^2 \sin^2\theta \ (d\varphi - \zeta(r) dt)^2 \right] \tag{2.8}$$

and $\Phi = \phi \ e^{i\omega_s t + in\varphi}$, where the metric components and the real function ϕ depend only on r and θ. The requirement that Φ is single-valued implies $n = 0, \pm 1, \pm 2, \ldots$. The solution has spherical symmetry for $n = 0$ and axial symmetry otherwise. Since the Lagrangian density is invariant under a global $U(1)$ transformation, the current, $j^\mu = -i\Phi^* \partial^\mu \Phi + \text{c.c.}$, is conserved and it is associated to a charge Q, satisfying the quantization condition with the angular momentum $J = nQ$ [37]. The numerical procedure to extract the metric and the scalar field is described in Ref. [33]. Throughout the paper we will consider solutions with $n = 2$, $b = 1.1$, $\lambda = 1.0$, $a = 2.0$ and different values of (J, M) corresponding to $J/(GM^2) \sim 0.566$, 0.731 and 0.858. In Fig. 4 the metric functions for a boson star along the equatorial plane are shown. By computing the coefficient g_{tt} one can prove that boson stars develop ergoregions deeply inside the star. For this particular choice of parameters, the ergoregion extends from $r/(GM) \sim 0.0471$ to 0.770. A more complete discussion on the ergoregions of rotating boson stars can be found in Ref. [33].

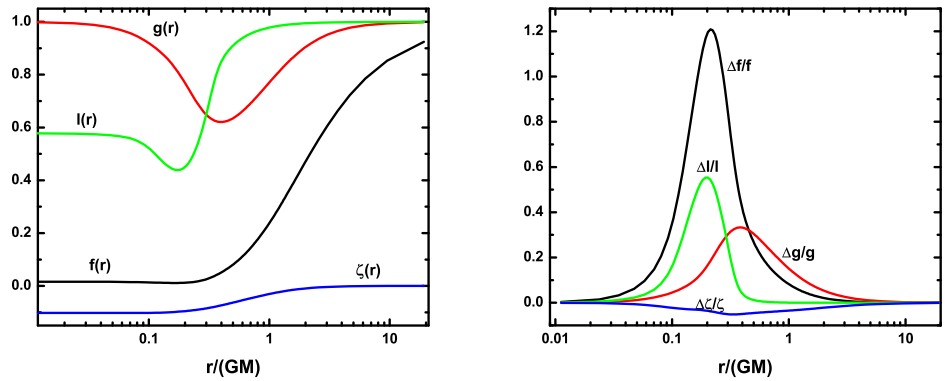

Figure 4: Left panel: Metric coefficients for a rotating boson star along the equatorial plane, with parameters $n = 2$, $b = 1.1$, $\lambda = 1.0$, $a = 2.0$, $J/(GM^2) \sim 0.566$. Right panel: Fractional difference of the metric potentials between $\theta = \pi/2$ and $\theta = \pi/4$ for the same star.

2.3 Ergoregion instability for rotating gravastars and boson stars

The stability of gravastars and boson stars can be studied perturbatively by considering small deviations around equilibrium. Due to the difficulty of handling gravitational perturbations for rotating objects, the calculations below are mostly restricted to scalar perturbations. However the equation for axial gravitational perturbations of gravastars is identical to the equation for scalar perturbations in the large $l = m$ limit [23]. There are also generic arguments suggesting that the timescale of gravitational perturbations is smaller than the timescale of scalar perturbations for low m [38]. Thus, scalar perturbations should provide a lower bound on the strength of the instability.

2.3.1 Scalar field instability for slowly rotating gravastars: WKB approach

Consider now a minimally coupled scalar field in the background of a gravastar. The metric of gravastars is given by Eq. (2.4). In the large $l = m$ limit, which is appropriate for a WKB analysis [32, 39], the scalar field can be expanded as

$$\Phi = \sum_{lm} \bar{\chi}_{lm}(r) \exp\left[-\frac{1}{2}\int\left(\frac{2}{r}+\frac{f'}{2f}+\frac{B'}{2B}\right)dr\right] e^{-i\omega t} Y_{lm}(\theta,\phi)\,. \tag{2.9}$$

The functions $\bar{\chi}_{lm}$ are determined by the Klein-Gordon equation which, dropping terms of order $\mathscr{O}\left(1/m^2\right)$, yields

$$\bar{\chi}''_{lm} + m^2 T(r,\Sigma)\bar{\chi}_{lm} = 0\,, \tag{2.10}$$

where $\Sigma \equiv -\omega/m$ and

$$T = \frac{B(r)}{f(r)}\left(\Sigma - V_+\right)\left(\Sigma - V_-\right), \qquad V_\pm = -\omega \pm \frac{\sqrt{f(r)}}{r}\,. \tag{2.11}$$

Equation (2.10) can be shown to be identical for the axial gravitational perturbations of perfect fluid stars [24].

The WKB method [32] for computing the eigenfrequencies of Eq. (2.10) is in excellent agreement with full numerical results [39]. The quasi-bound unstable modes are determined by

$$m\int_{r_a}^{r_b}\sqrt{T(r)}dr = \frac{\pi}{2} + n\pi\,, \quad n = 0,1,2,\ldots \tag{2.12}$$

and have an instability timescale

$$\tau = 4\exp\left[2m\int_{r_b}^{r_c}\sqrt{|T|}dr\right]\int_{r_a}^{r_b}\frac{d}{d\Sigma}\sqrt{T}dr\,, \tag{2.13}$$

where r_a, r_b are solutions of $V_+ = \Sigma$ and r_c is determined by the condition $V_- = \Sigma$.

Table 2 shows the WKB results for the anisotropic pressure model for different values of J/M^2. Although the WKB approximation breaks down at low m values, these results still provide reliable estimates [32]. This claim has be verified with a full numerical integration of the Klein-Gordon equation. The results show that the instability timescale decreases as the star becomes more compact. Larger values of J/M^2 make the star more unstable. The maximum growth time of the instability can be of the order of a few thousand M, but it crucially depends on J, μ and δ [36]. For a large range of parameters this instability is crucial for the star evolution. Gravitational

perturbations are expected to be more unstable. Moreover it is worth to notice that the slowly rotating approximation allows only for $\mu < 0.5$, while for rotating BHs $0.5 < \mu < 1$ (see Table 1). The ergoregion instability being monotonically increasing with μ, we expect that instability timescales for realistic gravastars should be much shorter than the ones computed. For most of the BH mimickers models to be viable we require $J/M^2 \sim 1$ and $\mu \sim 1$. It would be interesting to study whether the ergoregion instability is or is not always effective in this case. Possible future developments include: (i) a full rotating gravastar model, which allows for $\mu > 0.5$; (ii) the stability analysis against gravitational perturbations for rotating gravastars; (iii) a gravavastar model which is not strongly dependent on the thickness, δ.

The ergoregion instability of a rotating boson star is straightforwardly computed following the method described above for spinning gravastars. We refer the reader to [23] and we only summarize the results in Table 3. The maximum growth time for this boson star model is of the order of $10^6 M$ for $J/GM^2 = 0.857658$. Thus the instability seems to be truly effective for rotating boson stars.

Table 2: WKB results for the instability of rotating gravastars with $r_2 = 2.2$, $r_1 = 1.8$ and $M = 1$.

	τ/M				
	$J/M^2 = 0.40$	$J/M^2 = 0.60$	$J/M^2 = 0.80$	$J/M^2 = 0.90$	$J/M^2 = 1.0$
m	$\Omega/\Omega_K = 0.33$	$\Omega/\Omega_K = 0.49$	$\Omega/\Omega_K = 0.65$	$\Omega/\Omega_K = 0.74$	$\Omega/\Omega_K = 0.82$
1	1.33×10^7	2.78×10^4	5.99×10^3	3.58×10^3	2.34×10^3
2	8.25×10^7	1.14×10^6	1.11×10^5	4.81×10^4	2.33×10^4
3	1.31×10^{10}	5.65×10^7	2.25×10^6	6.82×10^5	2.45×10^5
4	2.50×10^{12}	2.95×10^9	4.81×10^7	1.02×10^7	2.73×10^6
5	5.06×10^{14}	1.59×10^{11}	1.02×10^9	1.52×10^8	3.07×10^7

Table 3: Instability for rotating boson stars with parameters $n = 2$, $b = 1.1$, $\lambda = 1.0$, $a = 2.0$ and different values of J (from [23]). The Newton constant is defined as $4\pi G = 0.05$.

	$\tau/(GM)$		
m	$J/GM^2 = 0.566139$	$J/GM^2 = 0.730677$	$J/GM^2 = 0.857658$
1	8.847×10^2	6.303×10^3	–
2	7.057×10^3	5.839×10^4	1.478×10^6
3	6.274×10^4	$9.274. \times 10^5$	2.815×10^8
4	5.824×10^5	1.603×10^7	2.815×10^{10}
5	5.554×10^6	2.915×10^8	1.717×10^{12}

3. A toy model for Kerr-like objects

This section discusses Kerr-like objects such as particular solutions of rotating wormholes and superspinars. A rigorous analysis of the ergoregion instability for these models is a non-trivial task.

Indeed known wormhole solutions are special non-vacuum solutions of the gravitational field equations, thus their investigation requires a case-by-case analysis of the stress-energy tensor. Moreover exact solutions of four-dimensional superspinars are not known. To overcome these difficulties, the following analysis will focus on a simple model which captures the essential features of most Kerr-like horizonless ultra-compact objects. Superspinars and rotating wormholes will be modeled by the exterior Kerr metric down to their surface, where mirror-like boundary conditions are imposed. This problem is very similar to Press and Teukolsky's "BH bomb" [29, 30], i.e. a rotating BH surrounded by a perfectly reflecting mirror with its horizon replaced by a reflecting surface. For a more detailed discussion see [24].

3.0.2 Superspinars and Kerr-like wormholes

A superspinar of mass M and angular momentum $J = aM$ can be modeled by the Kerr geometry [16]

$$ds^2_{\rm Kerr} = -\left(1-\frac{2Mr}{\Sigma}\right)dt^2+\frac{\Sigma}{\Delta}dr^2+\left[\frac{(r^2+a^2)}{\sin^2\theta}+\frac{2Mr}{\Sigma}a^2\right]\sin^4\theta d\phi^2-\frac{4Mr}{\Sigma}a\sin^2\theta d\phi dt+\Sigma d\theta^2\,, \tag{3.1}$$

where $\Sigma = r^2+a^2\cos^2\theta$ and $\Delta = r^2+a^2-2Mr$. Unlike Kerr BHs, superspinars have $a > M$ and no horizon. Since the domain of interest is $-\infty < r < +\infty$, the space-time possesses naked singularities and closed timelike curves in regions where $g_{\phi\phi} < 0$ [40]. High energy modifications (i.e. stringy corrections) in the vicinity of the singularity are also expected.

Kerr-like wormholes are described by metrics of the form

$$ds^2_{\rm wormhole} = ds^2_{\rm Kerr} + \delta g_{ab}dx^a dx^b\,, \tag{3.2}$$

where δg_{ab} is infinitesimal. In general, Eq. (3.2) describes an horizonless object with a excision at some small distance of order ε from the would-be horizon [15]. Wormholes require exotic matter and/or divergent stress tensors, thus some ultra-stiff matter is assumed close to the would-be horizon. In the following, both superspinars and wormholes will be modeled by the Kerr metric with a rigid "wall" at finite Boyer-Lindquist radius r_0, which excludes the pathological region.

3.1 Instability analysis

If the background geometry of superspinars and wormholes is sufficiently close to the Kerr geometry, its perturbations is determined by the equations of perturbed Kerr BHs [24]. Thus the instability of superspinars and wormholes is studied by considering Kerr geometries with arbitrary rotation parameter a and a "mirror" at some Boyer-Lindquist radius r_0. Using the Kinnersley tetrad and Boyer-Lindquist coordinates, it is possible to separate the angular variables from the radial ones, decoupling all quantities. Small perturbations of a spin-s field are reduced to the radial and angular master equations [41]

$$\Delta^{-s}\frac{d}{dr}\left(\Delta^{s+1}\frac{dR_{lm}}{dr}\right)+\left[\frac{K^2-2is(r-M)K}{\Delta}+4is\omega r-\lambda\right]R_{lm}=0\,, \tag{3.3}$$

$$\left[(1-x^2){}_sS_{lm,x}\right]_{,x}+\left[(a\omega x)^2-2a\omega sx+s+{}_sA_{lm}-\frac{(m+sx)^2}{1-x^2}\right]{}_sS_{lm}=0\,, \tag{3.4}$$

where $x \equiv \cos\theta$, $\Delta = r^2 - 2Mr + a^2$ and $K = (r^2+a^2)\omega - am$. Scalar, electromagnetic and gravitational perturbations correspond to $s = 0, \pm 1, \pm 2$ respectively. The separation constants λ and ${}_sA_{lm}$ are related by $\lambda \equiv {}_sA_{lm} + a^2\omega^2 - 2am\omega$.

3.1.1 Analytic results

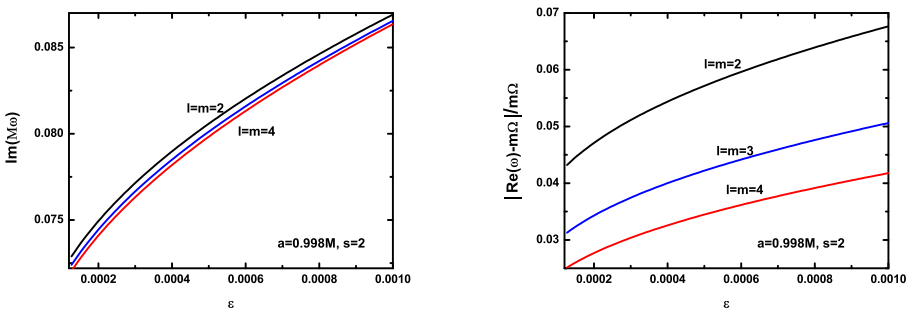

Figure 5: Imaginary and real parts of the characteristic gravitational frequencies for an object with $a = 0.998M$, according to the analytic calculation for rapidly-spinning objects. The mirror location is at $r_0 = (1+\varepsilon)r_+$. The real part is approximately constant and close to $m\Omega$, in agreement with the assumptions used in the analytic approach.

Following Starobinsky [27], equations (3.3)-(3.4) can be analytically solved in the slowly-rotating and low-frequency regime, $\omega M \ll 1$, and in the rapidly-spinning regime, where $r_+ \sim r_-$ and $\omega \sim m\Omega_h$, where $\Omega_h \equiv a/(2Mr_+)$ is the angular velocity at the horizon. The details of the analytic approximation are described in Ref. [24]. Analytic solutions for a star with $a = 0.998M$ are shown in Fig. 5 where gravitational perturbations are considered. The instability timescale for gravitational perturbations is about five orders of magnitude smaller than the instability timescale for scalar perturbations.

3.2 Instability analysis: numerical results

The oscillation frequencies of the modes can be found from the canonical form of Eq. (3.3)

$$\frac{d^2Y}{dr_*^2} + VY = 0\,, \tag{3.5}$$

where

$$Y = \Delta^{s/2}(r^2+a^2)^{1/2}R\,, \qquad V = \frac{K^2 - 2is(r-M)K + \Delta(4ir\omega s - \lambda)}{(r^2+a^2)^2} - G^2 - \frac{dG}{dr_*}\,, \tag{3.6}$$

and $K = (r^2+a^2)\omega - am$, $G = s(r-M)/(r^2+a^2) + r\Delta(r^2+a^2)^{-2}$. The separation constant λ is related to the eigenvalues of the angular equation by $\lambda \equiv {}_sA_{lm} + a^2\omega^2 - 2am\omega$. The eigenvalues ${}_sA_{lm}$ are expanded in power series of $a\omega$ as [42]

$${}_sA_{lm} = \sum_{k=0} f^{(k)}_{slm}(a\omega)^k\,. \tag{3.7}$$

Terms up to order $(a\omega)^2$ are included in the calculation. Absence of ingoing waves at infinity implies

$$Y \sim r^{-s} e^{i\omega r_*} . \tag{3.8}$$

Numerical results are obtained by integrating Eq. (3.5) inward from a large distance r_∞. The integration is performed with the Runge-Kutta method with fixed ω starting at $Mr_\infty = 400$, where the asymptotic behavior (3.8) is imposed. (Choosing a different initial point does not affect the final results.) The numerical integration is stopped at the radius of the mirror r_0, where the value of the field $Y(\omega, r_0)$ is extracted. The integration is repeated for different values of ω until $Y(\omega, r_0) = 0$ is obtained with the desired precision. If $Y(\omega, r_0)$ vanishes, the field satisfies the boundary condition for perfect reflection and $\omega = \omega_0$ is the oscillation frequency of the mode.

3.2.1 Objects with $a < M$

The regime $a < M$ requires a surface or mirror at $r_0 = r_+(1+\varepsilon) > r_+$. Thus the compactness is $M/r_0 \sim (1-\varepsilon)M/r_+$ and, in the limit $\varepsilon \to 0$, it is infinitesimally close to the compactness of a Kerr BH. Numerical results for scalar and gravitational perturbations of objects with $a < M$ are summarized in Table 4 and are in agreement with the analytic results [24]. The instability is weaker for larger m. This result holds also for $l \neq m$ and $s = 0$, ± 1 and ± 2. The minimum instability timescale is of order $\tau \sim 10^5 M$ for a wide range of mirror locations. Figure 6 shows the results for gravitational perturbations. Instability timescales are of the order of $\tau \sim 2 \div 6M$. Thus gravitational perturbations lead to an instability about five orders of magnitude stronger than the instability due to scalar perturbations (see Table 4). Figure 6 shows that the ergoregion instability remains relevant even for values of the angular momentum as low as $a = 0.6M$.

Table 4: Characteristic frequencies and instability timescales for a Kerr-like object with $a = 0.998M$. The mirror is located at $\varepsilon = 0.1$, corresponding to the compactness $\mu \sim 0.9\mu_{\rm Kerr}$.

	$(\mathrm{Re}(\omega)M, \mathrm{Im}(\omega)M)$	
$l = m$	$s = 0$	$s = 2$
1	$(0.1120, 0.6244 \times 10^{-5})$	–
2	$(0.4440, 0.5373 \times 10^{-5})$	$(0.4342, 0.2900)$
3	$(0.7902, 0.1928 \times 10^{-5})$	$(0.7803, 0.2977)$
4	$(1.1436, 0.5927 \times 10^{-6})$	$(1.1336, 0.3035)$

3.2.2 Objects with $a > M$

Objects with $a > M$ could potentially describe superspinars. Several arguments suggest that objects rotating above the Kerr bound are unstable. Firstly, extremal Kerr BHs are marginally stable. Thus the addition of extra rotation should lead to instability. Secondly, fast-spinning objects usually take a pancake-like form [43] and are subject to the Gregory-Laflamme instability [44, 45]. Finally, Kerr-like geometries, like naked singularities, seem to be unstable against a certain class of gravitational perturbations [46, 47] called algebraically special perturbations [40]. For objects

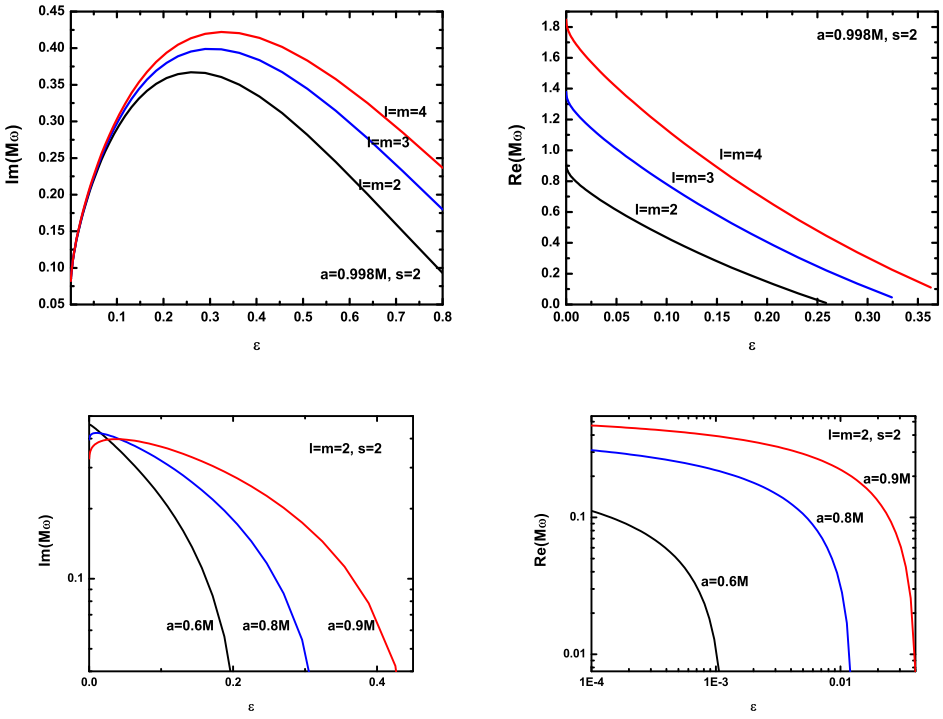

Figure 6: Details of the instability for gravitational perturbations, for different $l = m$ modes and $a/M = 0.998$ (top panels) and for $l = m = 2$ and different $a/M < 1$.

with $a > M$ the surface or mirror can be placed anywhere outside $r = 0$. In general the instability is as strong as in the $a < M$ regime. An example in shown in Fig. 7 for the surface at $r_0/M = 0.001$. This result confirms other investigations suggesting that ultra-compact objects rotating above the Kerr bound are unstable [48].

4. Conclusion

We investigated the ergoregion instability of some ultra-compact, horizonless objects which can mimick the spacetime of a rotating black hole. We studied some of the most viable BH mimickers: gravastars, boson stars, wormhole and superspinars.

If rotating, boson stars and gravastars may develop ergoregion instabilities. Analytical and numerical results indicate that these objects are unstable against scalar field perturbations for a large range of the parameters. Slowly rotating gravastars can develop an ergoregion depending on their angular momentum, their compactness and the thickness of their intermediate region. In a recent work [36] it has pointed out that slowly rotating gravastars may not develop an ergoregion. In the formation of the ergoregion for rotating gravastars an important role is played by the thickness (see Figure 3) which is not easily detectable. Thus further investigations are needed to better understand the ergoregion formation in physical resonable gravastar models.

The instability timescale for both boson stars and gravastars can be many orders of magnitude stronger than the instability timescale for ordinary stars with uniform density. In the large $l = m$

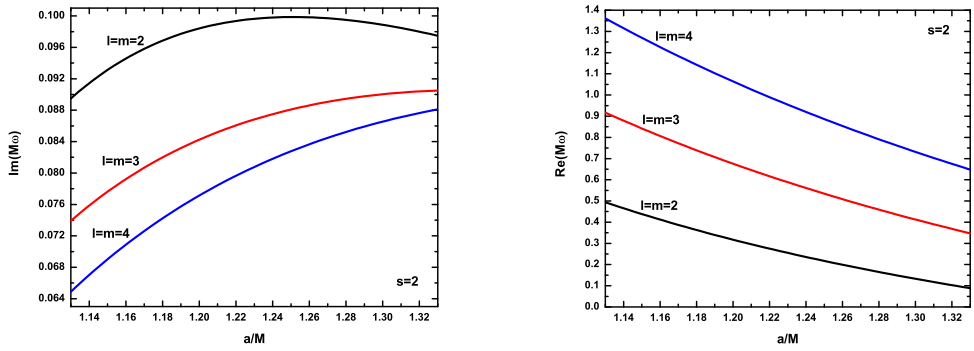

Figure 7: The fundamental $l = m = 2,3,4$ modes of an object spinning above the Kerr bound as function of rotation. The surface is located at $r_0/M = 0.001$.

approximation, suitable for a WKB treatment, gravitational and scalar perturbations have similar instability timescales. In the low-m regime gravitational perturbations are expected to have even shorter instability timescales than scalar perturbations. Instability timescales can be as low as ~ 0.1 seconds for a $M = 1M_\odot$ objects and about a week for supermassive BHs, $M = 10^6 M_\odot$, monotonically decreasing for larger rotations and a larger compactness.

The essential features of wormholes and superspinars have been captured by a simple model whose physical properties are largely independent from the dynamical details of the gravitational system. Numerical and analytic results show that the ergoregion instability of these objects is extremely strong for any value of their angular momentum, with timescales of order 10^{-5} seconds for a $1M_\odot$ object and 10 seconds for a $M = 10^6 M_\odot$ object. Therefore, high rotation is an indirect evidence for horizons.

Although further studies are needed, the above investigation suggests that exotic objects without event horizon are likely to be ruled out as viable candidates for astrophysical ultra-compact objects. This strengthens the role of BHs as candidates for astrophysical observations of rapidly spinning compact objects.

Acknowledgements

The authors warmly thank Matteo Losito for interesting discussions and for sharing some of his results. This work is supported by Fundação para a Ciência e Tecnologia (FCT) - Portugal through project PTDC/FIS/64175/2006 and by the National Science Foundation through LIGO Research Support grant NSF PHY-0757937.

References

[1] S. W. Hawking, Commun. Math. Phys. **25**, 152 (1972).

[2] R. Narayan, New J. Phys. **7**, 199 (2005).

[3] R. D. Blandford and R. L. Znajek, Mon. Not. Roy. Astron. Soc. **179**, 433 (1977).

[4] C. F. Gammie, S. L. Shapiro and J. C. McKinney, Astrophys. J. **602**, 312 (2004).

[5] J. M. Miller, A. C. Fabian, M. A. Nowak and W. H. G. Lewin, arXiv:astro-ph/0402101.

[6] R. Narayan, J. E. McClintock and R. Shafee, AIP Conf. Proc. **968** (2008) 265

[7] J. M. Wang, Y. M. Chen, L. C. Ho and R. J. McLure, Astrophys. J. **642**, L111 (2006).

[8] M. A. Abramowicz, W. Kluzniak and J. P. Lasota, Astron. Astrophys. **396**, L31 (2002).

[9] P. O. Mazur and E. Mottola, "Gravitational condensate stars," arXiv:gr-qc/0109035.

[10] C. B. M. Chirenti and L. Rezzolla, Class. Quant. Grav. **24**, 4191 (2007).

[11] C. Cattoen, T. Faber and M. Visser, Class. Quant. Grav. **22**, 4189 (2005).

[12] D. J. Kaup, Phys. Rev. **172**, 1331 (1968); R. Ruffini and S. Bonazzola, Phys. Rev. **187**, 1767 (1969).

[13] M. Visser, *Lorentzian wormholes: From Einstein to Hawking*, (American Institute of Physics, NY, 1995).

[14] J. P. S. Lemos, F. S. N. Lobo and S. Quinet de Oliveira, Phys. Rev. D **68**, 064004 (2003).

[15] T. Damour and S. N. Solodukhin, Phys. Rev. D **76**, 024016 (2007).

[16] E. G. Gimon and P. Horava, arXiv:0706.2873 [hep-th].

[17] S. W. Hawking, Phys. Rev. D **72** (2005) 084013 [arXiv:hep-th/0507171].

[18] R. Narayan, I. Yi and R. Mahadevan, Nature **374**, 623 (1995).

[19] A. E. Broderick and R. Narayan, Class. Quant. Grav. **24**, 659 (2007).

[20] M. Vallisneri, Phys. Rev. Lett. **84**, 3519 (2000).

[21] J. P. S. Lemos and O. B. Zaslavskii, Phys. Rev. D **76** (2007) 084030 [arXiv:0707.1094 [gr-qc]].

[22] J. P. S. Lemos and O. B. Zaslavskii, Phys. Rev. D **78** (2008) 024040 [arXiv:0806.0845 [gr-qc]].

[23] V. Cardoso, P. Pani, M. Cadoni and M. Cavaglia, Phys. Rev. D **77** (2008) 124044

[24] V. Cardoso, P. Pani, M. Cadoni and M. Cavaglia, Class. Quant. Grav. **25** (2008) 195010

[25] J. L. Friedman, Commun. Math. Phys. **63**, 243 (1978).

[26] Ya. B. Zel'dovich, Pis'ma Zh. Eksp. Teor. Fiz. **14**, 270 (1971) [JETP Lett. **14**, 180 (1971)]; Zh. Eksp. Teor. Fiz **62**, 2076 (1972) [Sov. Phys. JETP **35**, 1085 (1972)].

[27] A. A. Starobinsky, Zh. Eksp. Teor. Fiz **64**, 48 (1973) [Sov. Phys. JETP **37**, 28 (1973)];
A. A. Starobinsky and S. M. Churilov, Zh. Eksp. Teor. Fiz **65**, 3 (1973) [Sov. Phys. JETP **38**, 1 (1973)].

[28] J. D. Bekenstein and M. Schiffer, Phys. Rev. D **58**, 064014 (1998).

[29] W. H. Press and S. A. Teukolsky, Nature **238**, 211 (1972).

[30] V. Cardoso, O. J. C. Dias, J. P. S. Lemos and S. Yoshida, Phys. Rev. D **70**, 044039 (2004) [Erratum-ibid. D **70**, 049903 (2004)]; V. Cardoso and O. J. C. Dias, Rev. D **70**, 084011 (2004);
E. Berti, V. Cardoso and J. P. S. Lemos, Phys. Rev. D **70**, 124006 (2004).

[31] B. F. Whiting, J. Math. Phys. **30** (1989) 1301.

[32] N. Comins and B. F. Schutz, Proc. R. Soc. Lond. A **364**, 211 (1978).

[33] B. Kleihaus, J. Kunz and M. List, Phys. Rev. D **72**, 064002 (2005); B. Kleihaus, J. Kunz, M. List and I. Schaffer, Phys. Rev. D **77** (2008) 064025 [arXiv:0712.3742 [gr-qc]].

[34] J. B. Hartle, Astrophys. J. **150**, 1005 (1967); J. B. Hartle and K. S. Thorne, Astrophys. J. **153**, 807 (1968).

[35] B. F. Schutz and N. Comins, MNRAS **182**, 69 (1978).

[36] C. B. M. Chirenti and L. Rezzolla, Phys. Rev. D **78** (2008) 084011 [arXiv:0808.4080 [gr-qc]].

[37] F. E. Schunck and E. W. Mielke, in *Relativity and Scientific Computing*, edited by F. W. Hehl, R. A. Puntigam and H. Ruder (Springer, Berlin, 1996), p. 138.

[38] K. D. Kokkotas, J. Ruoff and N. Andersson, Phys. Rev. D **70**, 043003 (2004).

[39] V. Cardoso, O. J. C. Dias, J. L. Hovdebo and R. C. Myers, Phys. Rev. D **73**, 064031 (2006).

[40] S. Chandrasekhar, Proc. R. Soc. London, Ser. A **392**, 1 (1984); *The Mathematical Theory of Black Holes*, (Oxford University Press, New York, 1983).

[41] S. A. Teukolsky, Phys. Rev. Lett **29**, 1114 (1972); S. A. Teukolsky, Astrophys. J. **185**, 635 (1973).

[42] E. Berti, V. Cardoso and M. Casals, Phys. Rev. D **73**, 024013 (2006) [Erratum-ibid. D **73**, 109902 (2006).

[43] R. Emparan and R. C. Myers, JHEP **0309**, 025 (2003).

[44] R. Gregory and R. Laflamme, Phys. Rev. Lett. **70**, 2837 (1993).

[45] V. Cardoso and O. J. C. Dias, Phys. Rev. Lett. **96**, 181601 (2006); V. Cardoso and L. Gualtieri, Class. Quant. Grav. **23**, 7151 (2006); V. Cardoso, O. J. C. Dias and L. Gualtieri, arXiv:0705.2777 [hep-th].

[46] V. Cardoso and M. Cavaglià, Phys. Rev. D **74**, 024027 (2006).

[47] G. Dotti, R. Gleiser and J. Pullin, Phys. Lett. B **644**, 289 (2007).

[48] G. Dotti, R. J. Gleiser, I. F. Ranea-Sandoval and H. Vucetich, arXiv:0805.4306 [gr-qc].